

COMPLETENESS OF COMBUSTION AND CYCLIC EFFECTIVENESS IN SPARK-IGNITION ENGINES

Moshen Battoei –Avarzaman, Andrzej Sobiesiak

Department of Mechanical, Automotive and Material Engineering

University of Windsor, Windsor, ON, Canada N9B 3P4

Phone: 1-519-253 3000x.3886

e-mails: mbattoei@uwindsor.ca; asobies@uwindsor.ca

Abstract

The focus of this study was to apply and evaluate two separate techniques for estimating of the completeness of combustion in a multi-cylinder engine fueled with compressed natural gas. The degree of correlation between these two independent estimates of the combustion completeness was sought. One technique, with better time resolution and viewed to be more accurate, calculates the completeness of combustion and cyclic effectiveness on a cycle-by-cycle basis using in-cylinder pressure measurements. The technique utilizes the normalized pressure rise parameter due to combustion to describe the completeness of combustion. The second technique evaluates the completeness of combustion based on time-averaged measurements of unburned hydrocarbons in engine exhaust gases. Both the in-cylinder pressure and exhaust gas composition data were obtained from a test multi-cylinder engine fueled first with gasoline and then with compressed natural gas (CNG). The successful aspect of this investigation was to propose a new parameter, the cyclic effectiveness, that it is strongly related to completeness of combustion. The advantage of the new parameter is that its calculation does not require computations of the pressure rise due to combustion. It also avoids difficulties associated with that procedure in finding other parameters such as the polytropic exponents at the start and end of combustion.

1. Introduction

An important characteristic of internal combustion spark ignition engine is the non-repeatability of consecutive engine cycles. This feature is called cycle-to-cycle variation or cyclic dispersion. Due to cyclic dispersion, a fraction of the cycles will have lower efficiency and this will affect the average efficiency. It was pointed in [1] that elimination of cycle-to-cycle variation would result in a 10% increase in the power output for the same fuel consumption. The cycle-to-cycle variation manifests itself most clearly during the combustion period as the peak pressure, p_{max} , variation, and is frequently reported as the coefficient of variation, CoV, of the peak pressure. Rassweiler and Withrow's [2] analysis of cyclic variation is again focused on the combustion period and it calculates the referenced pressure rise, Ψ , due to combustion over the entire combustion period. Subsequently, under assumption of proportionality, the mass fraction burned (mfb) and its variability is calculated. However, the cyclic variation can be traced too much earlier processes of a) mixture formation and flow into the engine cylinder and turbulence in the inlet manifold, and b) early flame development after the spark event.

There is evidence [3] that the flow at the top dead center (TDC) is very sensitive to the velocity field in the cylinder at the moment of the intake valve closing, which is determined by the flow in the inlet manifold while the cylinder is filling. Thus, while the combustion on its own contributes to cyclic variability, the engine cycle-to-cycle variation could be defined to include pressures outside the combustion period. Stone [4] suggests that the indicated mean effective pressure (imep, which is calculated over the entire engine cycle) and the coefficient of variation is probably the parameter with most relevance to the overall performance of the engine.

Ball *et al* [4], [5], and later Al-Fakhri and Raine [6] report a good agreement between the experimental cycle-to-cycle variation data in terms of imep and p_{max} , and modeled data when using the distributions of experimental burn rate and a new parameter called completeness of combustion, X . This parameter was derived from the pressure rise due to combustion, Ψ .

In this paper, we examine the coefficients of variation of the peak pressure, $CoV_{p_{max}}$, the pressure rise over the combustion period CoV_{Ψ} , and the mean indicated pressure, CoV_{imep} , changes with two engine variables, spark timing and fuel to air ratio. We also sought for correlations between the respective coefficients of variation.

In addition, we propose that the distributions of indicated mean effective pressure and another parameter, the cycle effectiveness, R , based the average indicated mean effective pressure and a maximum from the distribution of the mean indicated pressures, could be used for characterization of cyclic variations and its simulation. The cyclic effectiveness, defined in such a way does include pressures from outside of the combustion period and avoids some arbitrary choices when calculations of the reference pressure rise, Ψ , are performed.

2. Experimental procedures

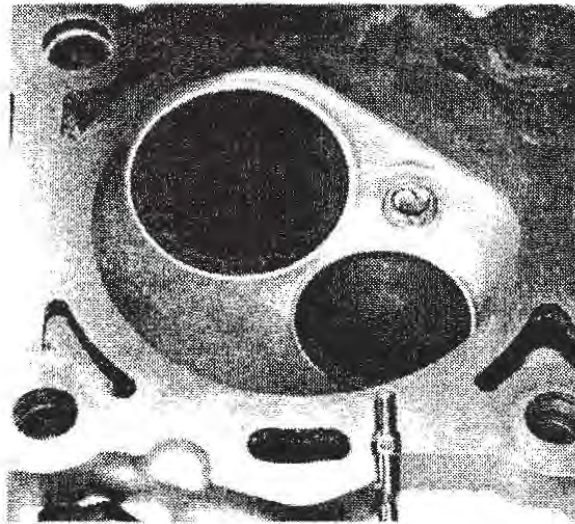


Fig. 1. Cylinder No. 1 combustion chamber showing the location of the wall mounted pressure transducer. The wall mounted transducer is shown removed from its mounting location in the cylinder head and is positioned directly above it for clarity (mounting hole not visible in this picture).

A DaimlerChrysler 4.7L V-8 test engine was used for the experimental measurements. The bore and stroke were 93 mm and 86.5 mm respectively with a compression ratio of 9.3:1. Figure 1 shows the configuration of cylinder No. 1's combustion chamber and the location of the wall mounted pressure transducer.

The wall mounted transducer was a Kistler 6052A1. This transducer was horizontally mounted into a specially machined cylinder head so that the transducer face was 4 mm recessed from the combustion chamber wall. It sat in a heavily cooled area of the cylinder head surrounded by cooling jackets and a thin layer of silicon coating was placed on the diaphragm to reduce the effects of thermal shock.

To collect and analyze the data from the transducer, an MTS Adapt-CAS system was used. The signal was first passed through the 1108 charge amplifier then connected to the 2816 12-bit analog to digital (A/D) board with sampling rate up to 1 MHz, which subsequently sent data to the 4344 module for calculations and logging.

Crankshaft Data Marker (CDM) and Pulses Per Revolution (PPR) signals were generated by an AVL encoder at 1-degree crank angle resolution throughout the cycle. The pressure data was comprised of acquiring and processing 270 consecutive cycles. In majority

of trials the engine speed and load were maintained constant at 1600 RPM and 394 mmHg (manifold absolute pressure), respectively even under very lean conditions when engine behavior was erratic. In CNG trials, the relative air to fuel ratio, λ , was varied within the range of 1.0 to 1.5. This was accomplished by adjusting injected fuel pulse width. The spark timing was also varied within the range of 18° to 48° . In gasoline trials, the relative air to fuel ratio, λ , was kept at constant value of 1. The spark timing was also varied within the range of 16° to 39° . A Horiba 7000 Series full exhaust analyzing system was used to sample and analyze the hydrocarbon exhaust emissions. The sampling point was connected to exhaust runner 1.

3. In-cylinder pressure data analysis

The analysis involves 270 cycles of in-cylinder pressure data acquired at each operating point. In Fig. 2 a typical pressure-volume trace is shown in logarithmic coordinates.

The combustion analysis program MTS Adapt -CAS locates peak pressure, p_{max} , and calculates the mfb, the imep, and the compression and expansion stroke polytropic indices, n_c and n_e . Means and higher moments of these variables distributions are calculated as well. Separate algorithms were used to calculate the normalized pressure rise due to combustion, Ψ , the statistical parameters of its distributions, and the combustion completeness parameter, X .

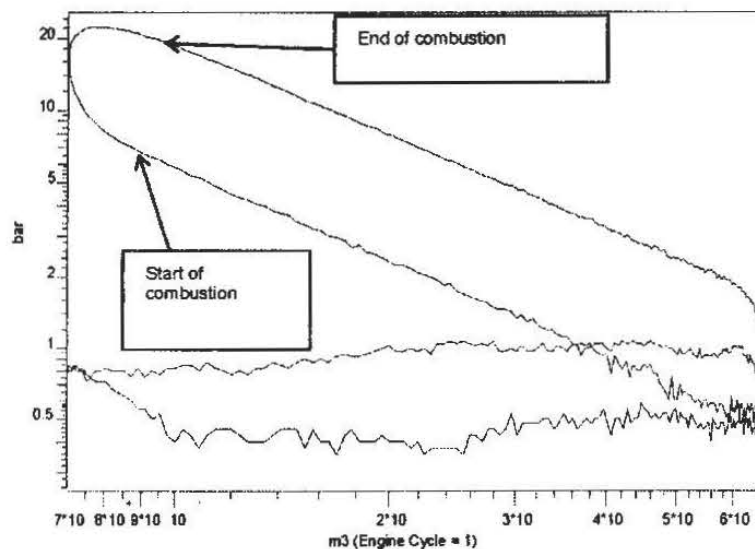


Fig. 2. In-cylinder measured pressure-volume trace in $\ln P$ and $\ln V$ coordinates.

The volume referenced pressure rise due to combustion Ψ and X are calculated as follows:

$$\Psi = \sum \Delta p^*$$

where Δp^* is referenced by volume pressure increments due to combustion.

$$X = \Psi / \Psi_m,$$

where Ψ_m is the maximum value from the referenced pressure rise Ψ distribution and it represents the most complete combustion cycle at given operating condition. The methodology to calculate Ψ and X in this investigation follows the procedure which is given in papers by Ball et al [4 and 5].

The Rassweiler and Withrow method takes nominal spark timing as the start of combustion and requires that an arbitrary choice of the combustion end is made (see Fig. 2). In addition several assumptions are introduced a) the referenced pressure rise due to combustion is proportional the mass fraction burned in each volume increment, b) there is allowance for heat transfer, combustion products dislocation or composition change.

Furthermore, the method strongly depends on using an appropriate value of the polytropic index, n . In Fig. 3, variations in polytropic indices for before and after the combustion period are shown within one set of 90 consecutive cycles.

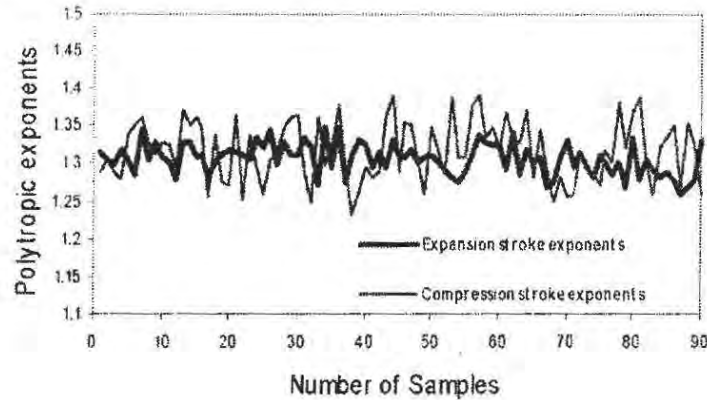


Fig. 3. Compression and expansion stroke polytropic indices variation at given operating point.

$$\bar{n}_e = 1.32 \quad \text{and} \quad STD = 0.04, \quad \bar{n}_c = 1.30 \quad \text{and} \quad STD = 0.02.$$

It is evident that the average indices and their standard deviations for the compression and expansion strokes have different values and they vary from cycle to cycle. These ambiguities prompted us to formulate a cyclic effectiveness parameter, R :

$$R = \text{imep} / \text{imep}_{\max},$$

where imep_{\max} is the maximum value from the imep distribution at given condition and it represents the most effective cycle (including combustion) within the distribution. The above definition of R does include individual pressure contributions over the entire cycle throughout the imep calculations and it captures the combustion impact in the imep_{\max} . It is important to point that calculation of the imep does not involve polytropic indices calculations and any of the arbitrary choices, which are necessary in the X computations.

Ball *et al* [4], [5] show how the average completeness of combustion, X , can be correlated with the unburned exhaust gas hydrocarbons, and we completed such measurements. Using the measured average hydrocarbon concentration $[\text{HC}]_{\text{exh}}$ and the measured average intake fuel concentration $[\text{HC}]_{\text{in}}$ the value η_{HC} is calculated, that represents the input fuel conversion efficiency:

$$\eta_{\text{HC}} = 1 - [\text{HC}]_{\text{exh}} / [\text{HC}]_{\text{in}}.$$

The η_{HC} fuel conversion efficiency does not include fraction of the fuel that only partially oxidized to carbon monoxide. However, as shown in [4] and [5], the η_{HC} is related to the average completeness of combustion, X , (and only with respect to fuel that completely oxidized to carbon dioxide) and it is anticipated that it is related to the cyclic effectiveness introduced in this study, R .

3. Experimental results and discussion

The evolution of probability density functions of Ψ , imep and p_{\max} with an increase of the relative air to fuel ratio, λ , and spark timing crank angle as parameter are shown in Figures 4 to 6 for fuelling with CNG. The mean and the maximum values of the Ψ and imep from

their respective distributions are used to calculate the combustion completeness X , and the cyclic effective R , respectively. The distributions maximum values and their spread vary with the change of operating condition.

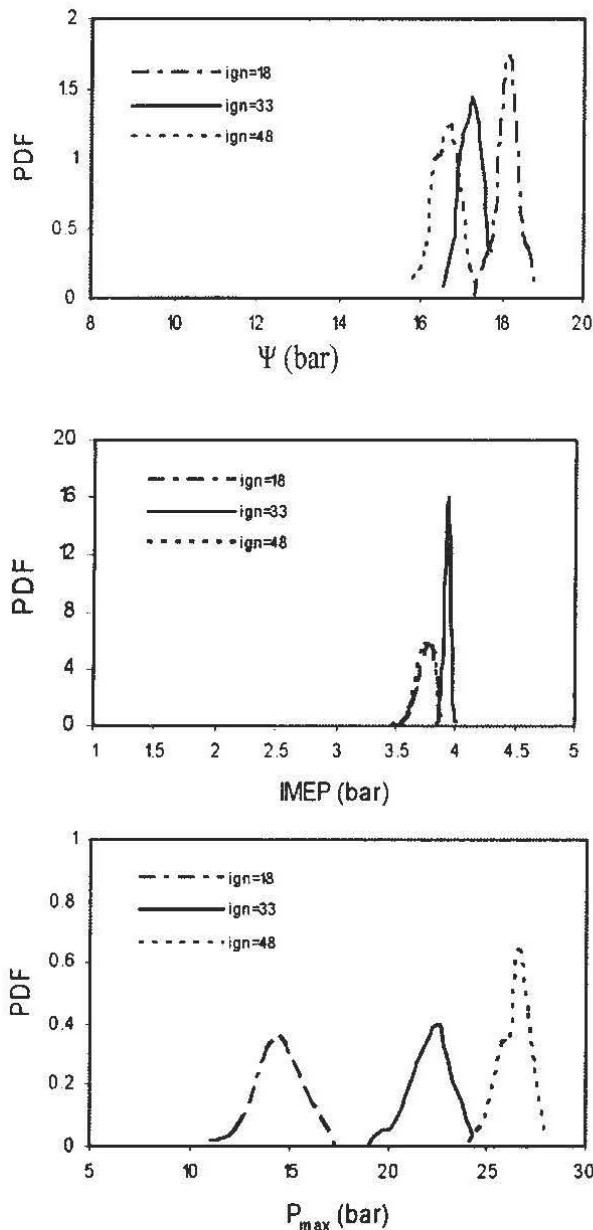


Fig. 4. Probability Density Function of Ψ , imep and p_{max} at $\lambda = 1.0$ and for three spark ignition timings.

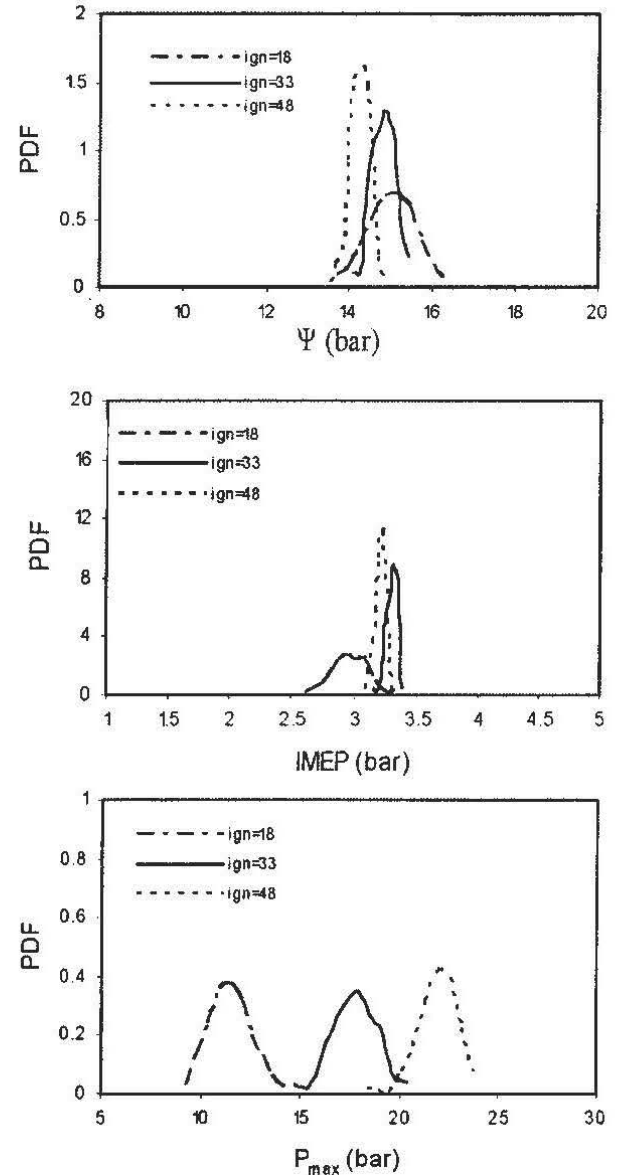


Fig. 5. Probability Density Function of Ψ , imep and p_{max} at $\lambda = 1.3$ and for three spark ignition timings.

One can notice that the PDF of imep distributions are at maximum and narrowly spread for the spark timing corresponding to best torque for given lambda (e.g. at 33° crank angle for $\lambda = 1.0$ in Fig. 4, or 48° crank angle for $\lambda = 1.3$ in Fig. 5.). Such a trend is less obvious in the Ψ distributions, where a continuous broadening of distributions with spark timing occurs. However, for the stoichiometric ($\lambda = 1$ in Fig. 4) and moderately lean ($\lambda = 1.3$ in Fig. 5) engine operation the PDFs of Ψ are better separated than the PDFs of imep for different values of ignition timing. This is a consequence of the fact that the calculations of Ψ include only combustion portion of the pressure trace, while the calculations of imep include pressures from the entire cycle. Both, the Ψ and imep PDF distributions become broader with the increase of lambda regardless the spark timing.

The general similarity of the Ψ and the imep PDF distributions suggests that they can be used interchangeably in deriving parameters to characterize cycle-to-cycle variation or completeness of combustion.

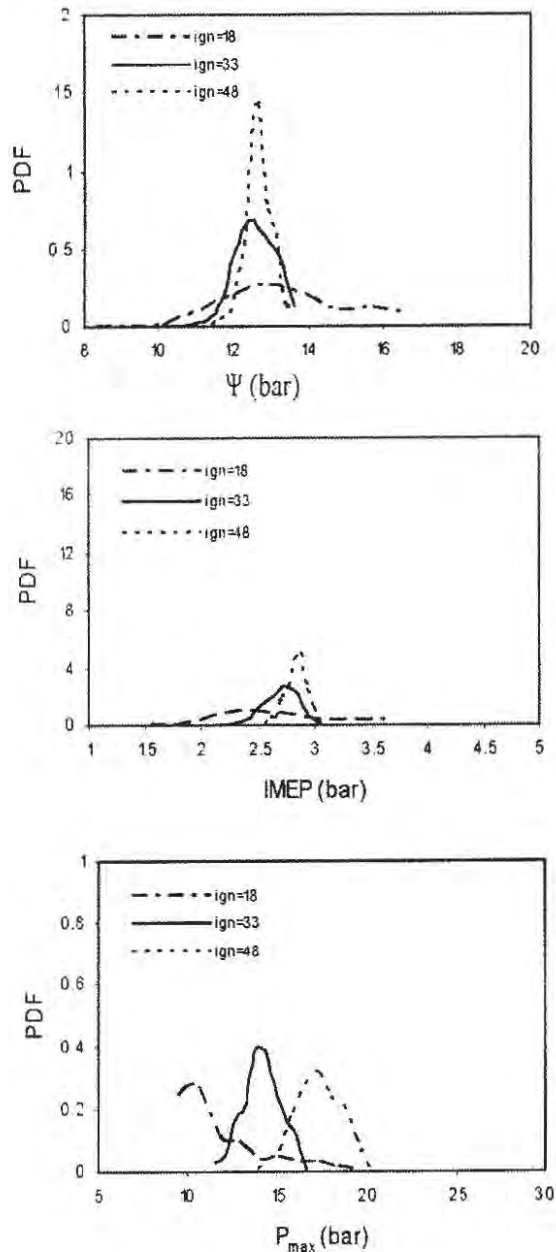


Fig. 6. Probability Density Function of Ψ , imep and p_{max} at $\lambda = 1.5$ and for three spark ignition timings.

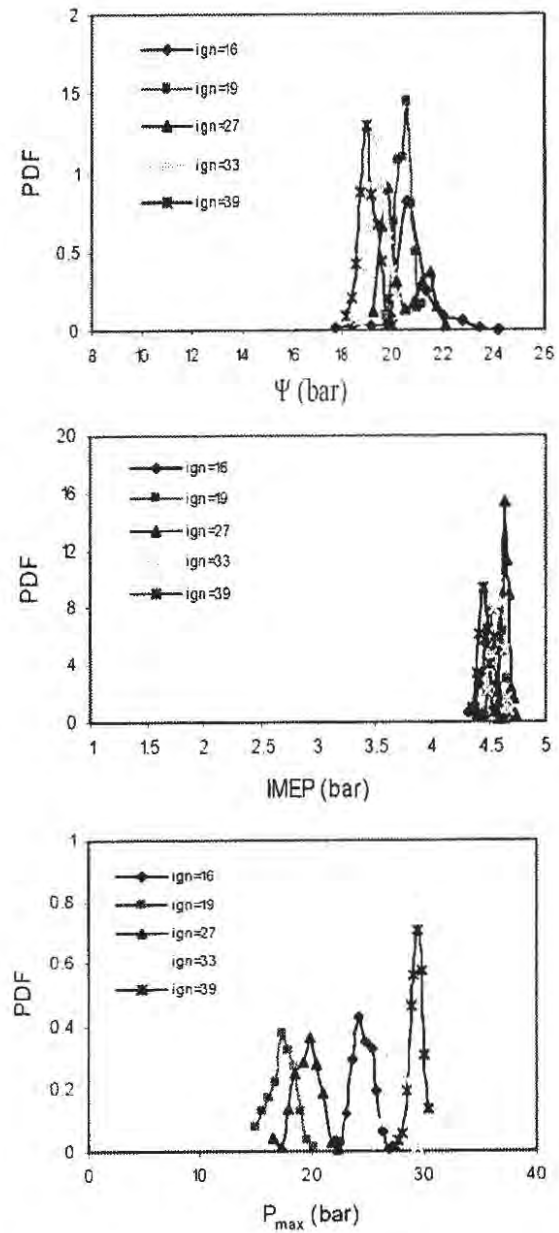


Fig. 7. Probability Density Function of Ψ , imep and p_{max} at $\lambda = 1.0$ and for several spark ignition timings. Engine fuelled with gasoline.

Figure 7 depicts the probability density functions of Ψ , imep and p_{max} for lambda one and several spark ignition timings for engine fuelling with gasoline.

The trends in PDF shapes are similar to those observed for CNG fuelling; the distributions of Ψ are boarder, while the PDF of imep peaks for spark timing at best torque. The best torque spark timing is now at lower value of the spark timing (27°) as indicated by the peak of PDF. The unexpected result is a bimodal distribution of the PDF of Ψ (pressure

rise due to combustion) at the spark timing of 27° . In contrast, the imep distribution at this operating point is a single-peaked, normal distribution. The trends observed in the PDF distributions can be re-examined by means of correlations between the coefficient of variation (CoV) of p_{\max} , Ψ , and imep for all spark timing and relative air to fuel ratio (λ - lambda).

The best fit lines in all subsequent figures are for the same spark timing and three different lambda values ($\lambda = 1.0, 1.3$ and 1.5). However, at the spark timing 18° and $\lambda = 1.5$ the engine misfired frequently, and in the graphs the results for this spark timing and this lambda only are replaced with the data for the spark timing of 28° (as marked in the figures). In the figures lambda values are indicated only along the 18° spark timing line, and they progress along the remaining spark timing lines in the same order. For well-correlated variables, the data points should line up along the graphs diagonal, or follow the same trend line. The CoV data for the p_{\max} and Ψ in Fig. 8, and the p_{\max} and imep in Fig. 9, correlate poorly.

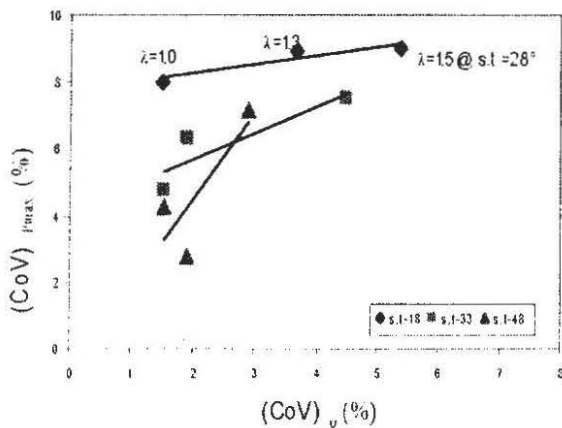


Fig. 8. The cycle maximum pressure cycle-to-cycle variations versus the completeness of combustion cycle-to-cycle variations for all operating conditions.

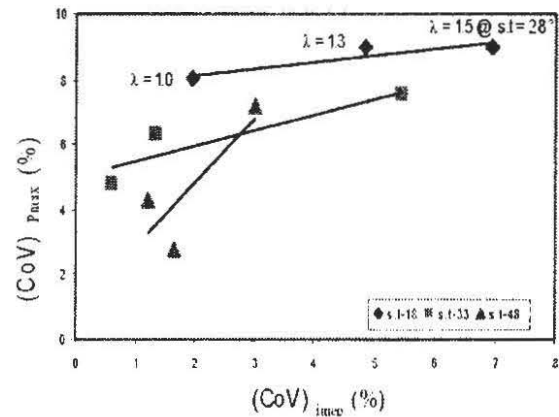


Fig. 9. The cycle maximum pressure cycle-to-cycle variations versus the indicated mean effective pressure cycle-to-cycle variations for all operating conditions.

In Fig. 10 the CoV of Ψ versus the CoV of imep is depicted and good correlation is demonstrated. This observation corroborates the hypothesis that the imep distribution contains as much information about combustion period as the Ψ distribution does. The results in the figures also indicate that leaning of the charge increases coefficient of variation while the CoV of the examined parameters are not sensitive to the spark timing. Fig. 11 presents the correlation between R , the cyclic effectiveness parameter, and X , the combustion completeness parameter. When examining results in Fig. 11, it is important to keep in mind that R is the imep normalized by $imep_{\max}$ for the R distribution, and X is the Ψ normalized by the Ψ_{\max} for the Ψ distribution. The normalization of both, the imep and Ψ , by their respective maximum values modifies the correlation illustrated in Fig. 10. The data correlates well and is gathered around the diagonal for all operating conditions. However, the cyclic effectiveness, R , seems to be more sensitive to the relative air to fuel ratio, λ , and to the spark timing. This result points at the impact of the normalization parameter. Al-Fekhri and Raine [6] postulate that the combustion completeness, X , which employs Ψ_m , does remove the spark timing effect from the results. Thus the scatter of the data is mostly in the R axis direction due to use of the $imep_{\max}$ in the R parameter definition.

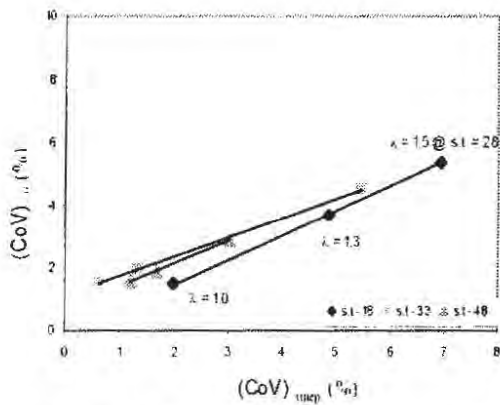


Fig. 10. The completeness of combustion cycle-to-cycle variations versus the indicated mean effective pressure cycle-to-cycle variations for all operating conditions

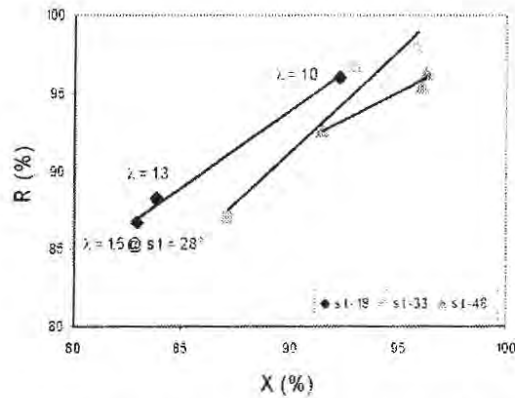


Fig. 11. The averaged cyclic effectiveness correlated against the averaged completeness of combustion for all operating conditions

In Fig. 12 the averaged completeness of combustion, X , is plotted against the fuel conversion efficiency, η_{HC} , and then in Fig. 13 the averaged cyclic effectiveness, R , versus, the fuel conversion efficiency, η_{HC} . The averaged value of R , X , and η_{HC} decrease as the mixture becomes leaner with increasing relative air to fuel ratio, λ . This correlates with increased coefficients of variation of the same parameters in Figs 8, 9, and 10. In Fig. 13 the data points correlate somewhat better than in Fig. 12 (the data points are closer to the graph's diagonal), suggesting that the cyclic effectiveness parameter, R , closer reflects input fuel conversion than the combustion completeness, X .

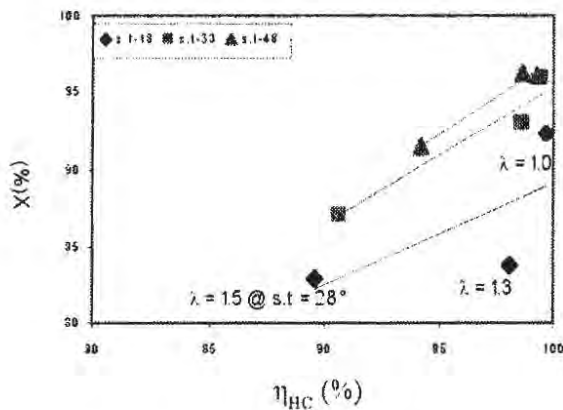


Fig. 12. The averaged completeness of combustion plotted against the fuel averaged conversion efficiency for all operating conditions

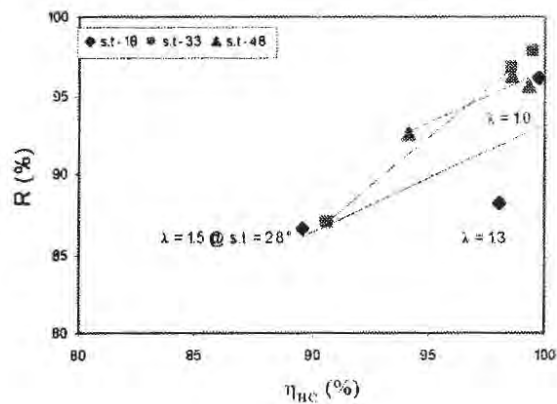


Fig. 13. The averaged cyclic effectiveness plotted against the fuel averaged conversion efficiency for all operating conditions.

4. Conclusion

We have demonstrated the following:

1. The newly defined parameter, R , called cyclic effectiveness, captures the cycle-to-cycle variations in SI engines and thus provides an alternative estimate of the cyclic variations.
2. The cyclic effectiveness parameter, R , correlates well with the combustion completeness parameter, X , suggesting that R could be alternatively used in cycle-to-

- cycle simulations.
3. The calculation of the cyclic effectiveness parameter avoids several assumptions and arbitrary chosen variables necessary when calculation of the combustion completeness is performed.
 4. The cyclic effectiveness parameter, R , correlates with the fuel conversion efficiency parameter, η_{HC} , equally good as the combustion completeness parameter, X .

5. Acknowledgments

The financial support of the Natural Science and Engineering Council, DaimlerChrysler Canada, and the University of Windsor School of Graduate Studies is gratefully acknowledged.

References

- [1] Stone, C. R. "Introduction to internal combustion engines." Third edition, SAE 2000
- [2] Rassweiler, G. M. and Withrow, L., "Motion pictures of engine flame correlated with pressure cards", SAE Paper 800131 (originally presented in 1938).
- [3] Reuss, D. L., Kuo, T. -W, Khaligi, B., Haworth, D., and Rosalik, M., "Particle image velocimetry measurements in a high swirl engine used for evaluation of computational fluid dynamics calculations.", SAE 952381, 1995.
- [4] Ball, J. K., Raine, R. R. and Stone C. R., "Combustion analysis and cycle-to-cycle variations in spark ignition engine combustion. Part 1: an evaluation of combustion analysis routines by reference to model data.", Proc. Instn. Mech. Engrs., Vol. 212, pp.381-399, 1998.
- [5] Ball J. K., Raine R. R. and Stone C. R., "Combustion analysis and cycle-to-cycle variations in spark ignition engine combustion. Parts 2: a new parameter for completeness of combustion and its use in modeling cycle-to-cycle variations in combustion.", Proc. Instn. Mech. Engrs., Vol. 212, pp.381-399, 1998.
- [6] Ball J. K., Raine R. R. and Stone C. R., "Combustion analysis and cycle-to-cycle variations in spark ignition engine combustion. Parts 2: a new parameter for completeness of combustion and its use in modeling cycle-to-cycle variations in combustion.", Proc. Instn. Mech. Engrs., Vol. 212, pp.381-399, 1998.
- [7] Al-Fakhri, Y. and Raine, R. R., "Application of a new technique for the evaluation of the cycle-by-cycle variation of completeness of combustion to changes of compression ratio.", SAE 2000-01-1213, 2000.